Ultrafast electronic processes at semiconductor polymer heterojunctions

A molecular-level, quantum-dynamical perspective

Irene Burghardt

Département de Chimie, Ecole Normale Supérieure, Paris

nanoSEMINAR TU Dresden

Acknowledgments & Collaborations

- Hiroyuki Tamura (ENS Paris)
- Eric R. Bittner (University of Houston)

Other collaborations:

- Lorenz Cederbaum, Etienne Gindensperger (University of Heidelberg)

Outline

- **Introduction:**
  Photophysics of organic semiconductors
- **Phonon-driven electronic processes in many dimensions:**
  Conical intersections and effective-mode models
- **Ultrafast exciton dissociation at polymer heterojunctions:**
  A molecular, quantum-dynamical perspective

Photophysics of organic semiconductors

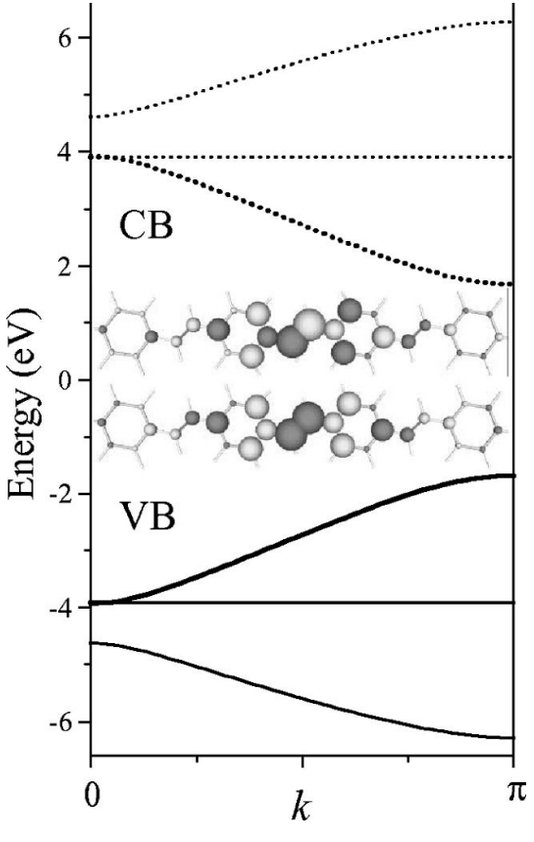

Karabunarliev, Bittner, J. Chem. Phys. 118, 4291 (2003)

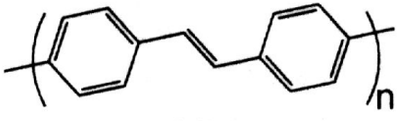

PPV

HOMO = valence band
LUMO = conduction band

- **delocalized electronic states, i.e., excitons, as in lattice structures**
- **ultrafast electronic processes involving exciton states**
- **coupling of electronic transitions to phonon modes/local modes**

Semiconducting polymer based devices

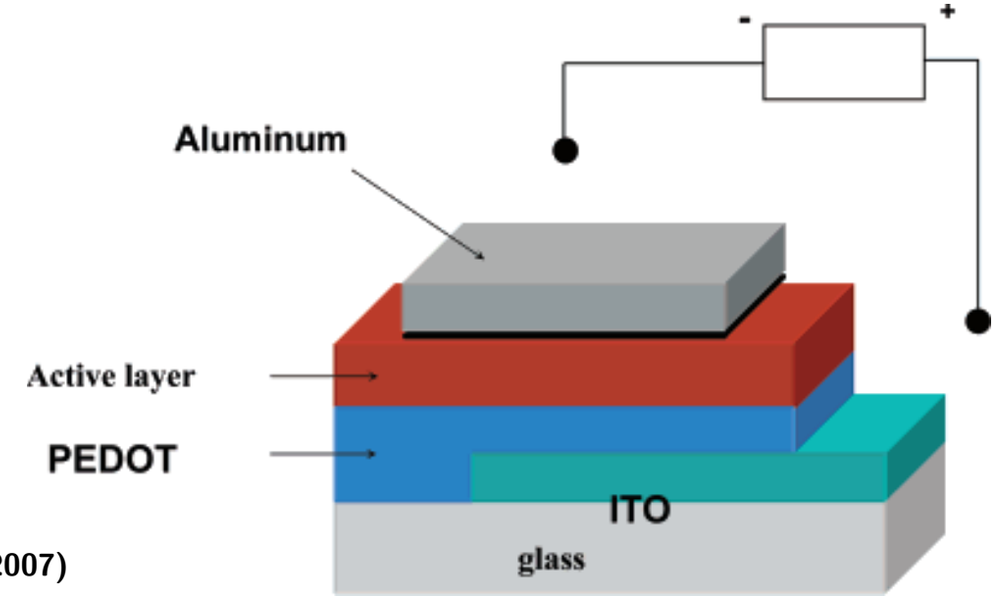

Gunes et al., Chem. Rev. 107, 1324 (2007)

OLED ↓

charge injection
charge transport
recombination → excitons
radiative decay of excitons

↑ **photovoltaic element**

Bulk heterojunctions

Highly efficient exciton dissociation sites

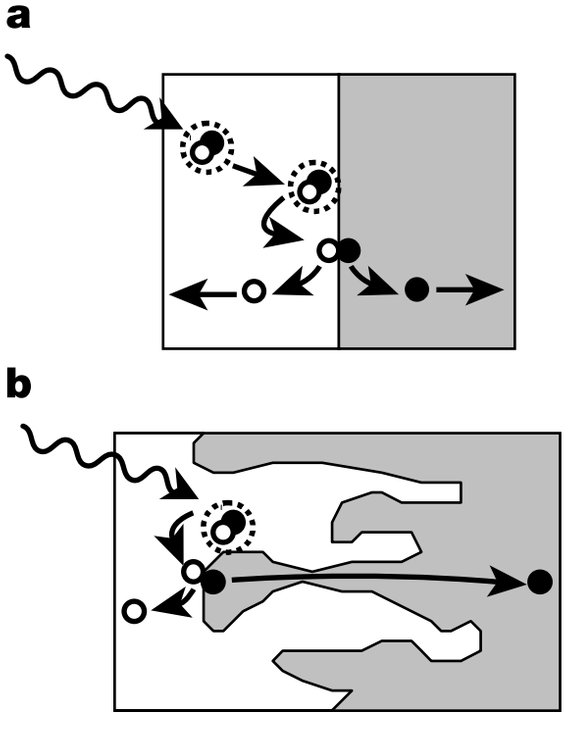

(a) bilayer cell
(b) bulk heterojunction cell

Peumans, Uchida, Forrest, Nature 125, 8098 (2003)

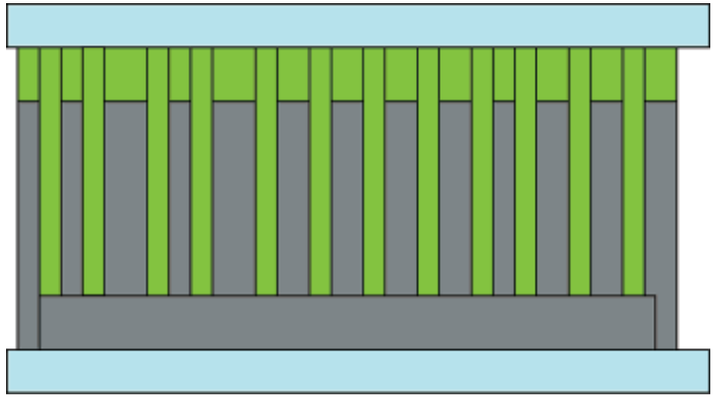

ideal structure of bulk heterojunction solar cell

Gunes et al., Chem. Rev. 107, 1324 (2007)

Photoluminescent vs. photovoltaic behavior

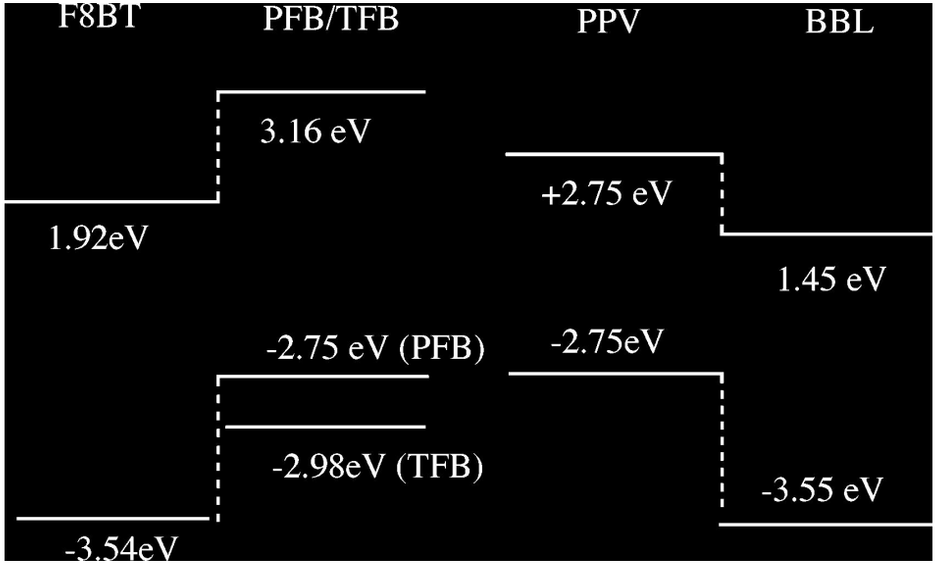

Ramon, Bittner, J. Phys. Chem. 110, 21001 (2006)

compare band offset ΔE with exciton binding energy ϵ_B ($\simeq$ 0.5 eV):

- if $\Delta E > \epsilon_B$: efficient charge separation, i.e., photovoltaic behavior
- if $\Delta E < \epsilon_B$: exciton state is stable, i.e., photoluminescent behavior
- if $\Delta E \simeq \epsilon_B$: more complicated intermediate case, e.g., TFB:F8BT

Time-resolved photoluminescence experiments

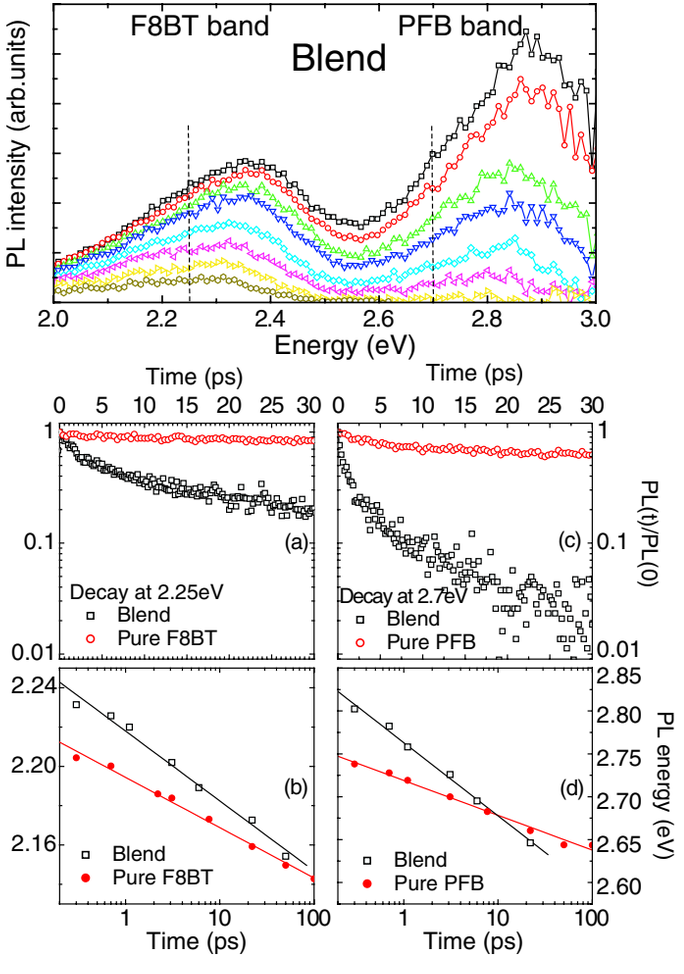

- picosecond scale decay of photoluminescence in the blend
- observation of exciton regeneration
- besides the band offset, polymer orientation at the heterojunction is a key factor

Sreearunothai et al., Phys. Rev. Lett. 96, 117403 (2006)

Morteani et al., Phys. Rev. Lett. 92, 247402 (2004)

Photoinduced processes at polymer heterojunctions

TFB:F8BT heterojunction

Tamura, Bittner, Burghardt
JCP 126, 021103 (2007)

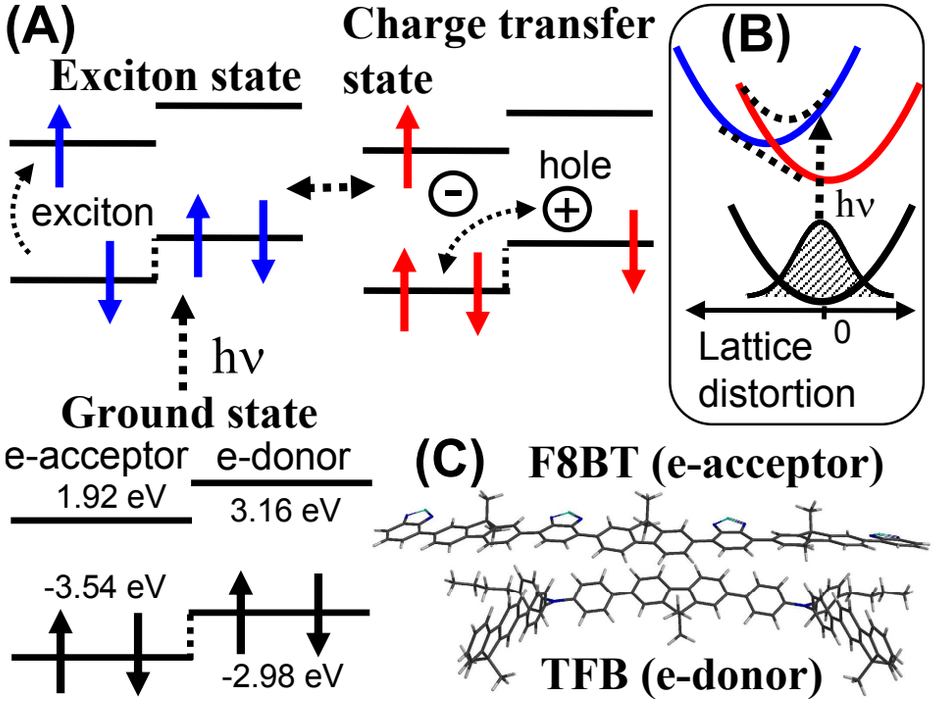

- initial photogeneration of an exciton state ("bright" state)
- exciton decay to an interfacial charge transfer state (exciplex)
- possible exciton regeneration at the heterojunction

Molecular picture: the TFB:F8BT heterojunction

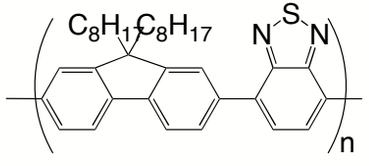

F8BT

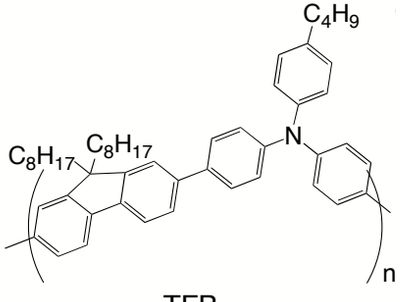

TFB

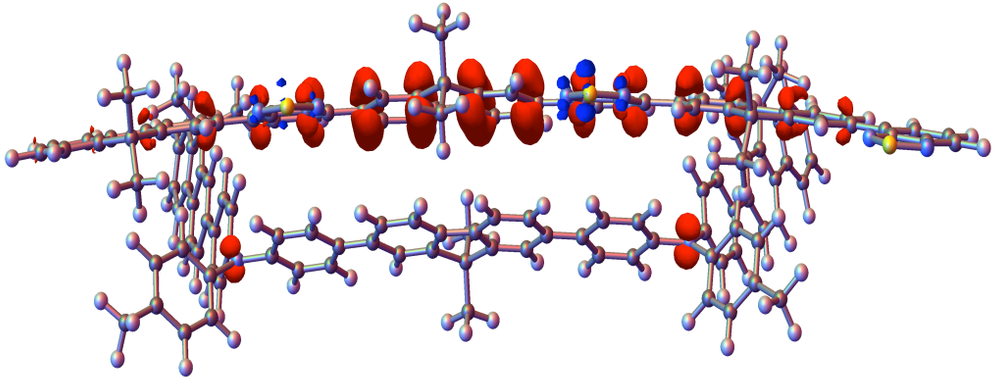

Ramon, Bittner, J. Phys. Chem. 110, 21001 (2006), J. Chem. Phys. 126, 181101 (2007)

semiempirical (PM3) and TD-DFT calculations

- **lowest excited state: charge transfer (CT) state: $TFB^{+}F8BT^{-}$ ("dark" state)**
- **lowest excited state with significant oscillator strength: exciton (XT) state on F8BT**

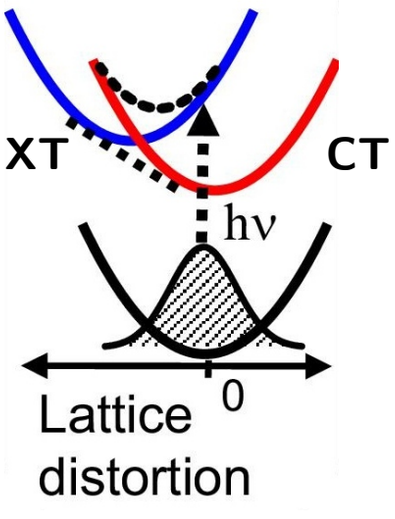

- **Can one obtain a molecular-level understanding of the processes at the heterojunction?**
- **How can the ultrafast nature of the exciton decay be explained?**
- **What is the role of electron-phonon coupling?**

- **Introduction:**
  Photophysics of organic semiconductors

- **Phonon-driven electronic processes in many dimensions:**
  Conical intersections and effective-mode models

- **Ultrafast exciton dissociation at polymer heterojunctions:**
  A molecular, quantum-dynamical perspective

Landmark topology: conical intersections (CIs)

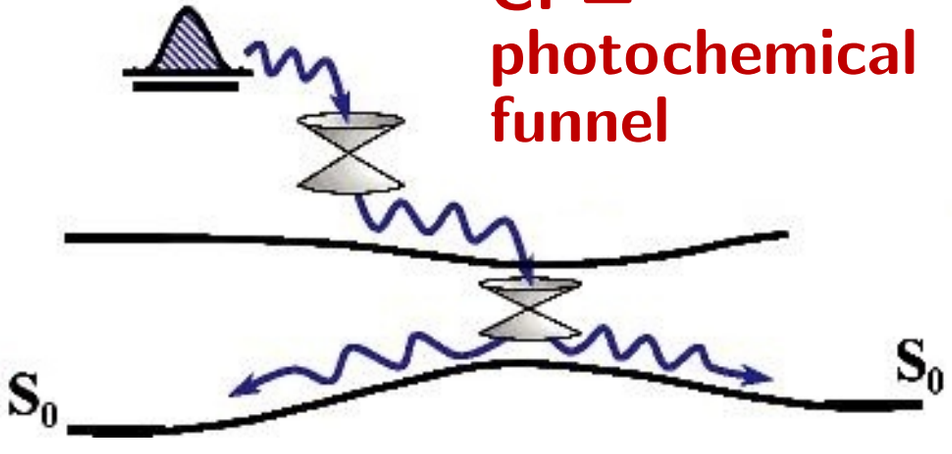

adapted from: Schultz et al., J. Am. Chem. Soc. 125, 8098 (2003)

- Conical intersection topologies are highly anharmonic
- Extreme breakdown of the Born-Oppenheimer approximation
- The electronic decay at a CI is ultrafast (femtosecond to picosecond scale)
- CIs are ubiquitous (Truhlar/Mead: "Principle of non-rareness of CIs")
- Polyatomic molecules; Jahn-Teller effect in solids

Basic model: linear vibronic coupling (LVC)$^{(*)}$

$$V_{\mathrm{CI}}(x_t, x_c) = V_0(x_t^0, x_c^0) + \begin{pmatrix} \kappa^{(1)}\,\Delta x_t & \lambda\,\Delta x_c \\ \lambda\,\Delta x_c & \kappa^{(2)}\,\Delta x_t \end{pmatrix}$$

$\Delta x_t = x_t - r_t^0$ **tuning mode**

$\Delta x_c = x_c - x_c^0$ **coupling mode**

2 dimensions: CI point
3 dimensions: CI seam
N dimensions: (N-2) dimensional intersection space

$^{(*)}$**here, diabatic representation**

$^{(*)}$**can be embedded in a correct representation of the overall potential via regularized diabatic states (Köppel).**

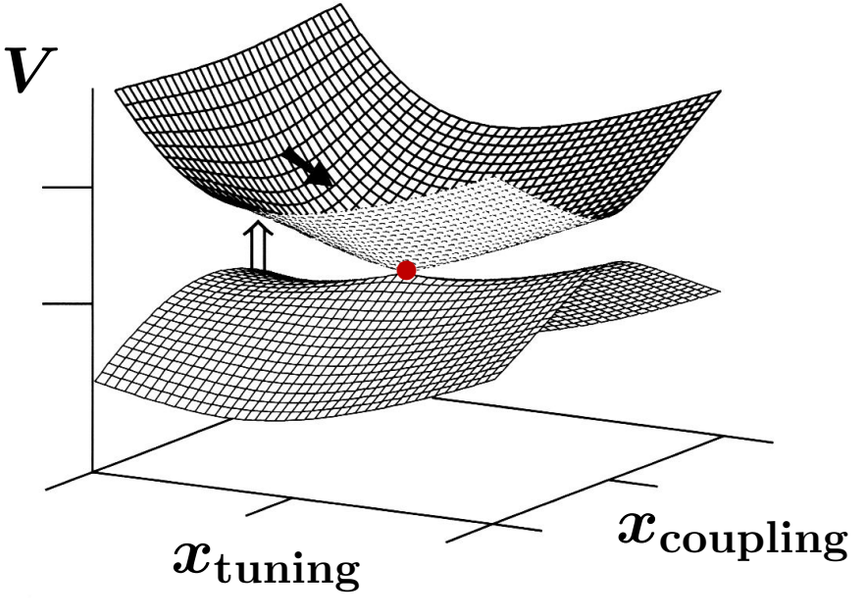

Dynamics at CIs in many dimensions

In view of the complicated CI topology:

Are "reduced" descriptions feasible at all?

Two strategies:

Strategy 1: explicit multi-dimensional quantum calculations

Strategy 2: define (few) effective modes, constructed so as to describe the short-time dynamics correctly

Strategy 1: explicit multidimensional dynamics

to solve the time-dependent Schrödinger equation: $i\hbar\dot{\Psi} = \hat{H}\Psi$

(or the Liouville-von-Neumann equation: $i\hbar\dot{\hat{\rho}} = \hat{\hat{L}}\hat{\rho}$)

$$\Psi(\mathrm{r},t) = \sum_J A_J(t)\Phi_J(\mathrm{r},t)$$

$$\text{with} \quad \Phi_J(\mathrm{r},t) = \prod_{\kappa=1}^{M} \varphi_{j_\kappa}^{(\kappa)}(\mathrm{r}_\kappa,t)$$

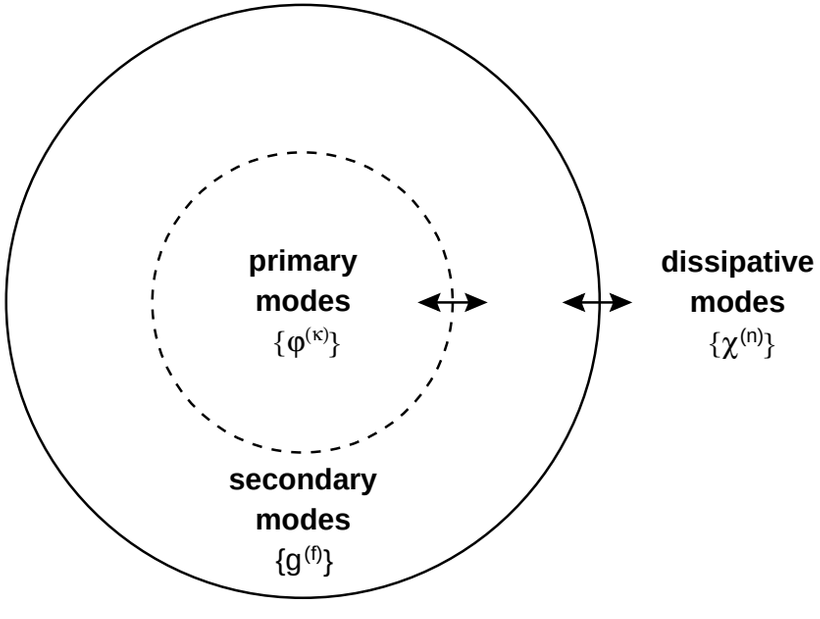

Multi-Configuration Time-Dependent Hartree (MCTDH)

cf. Meyer and co-workers, Phys. Rep. 324, 1 (2000)

Gaussian-based hybrid method: G-MCTDH

$$\Phi_J(\mathrm{r},t) = \underbrace{\prod_{\kappa=1}^{M} \varphi_{j_\kappa}^{(\kappa)}(\mathrm{r}_\kappa,t)}_{\text{primary modes}} \underbrace{\prod_{\kappa=M+1}^{P} g_{j_\kappa}^{(\kappa)}(\mathrm{r}_\kappa,t)}_{\text{secondary modes}}$$

Burghardt, Meyer, Cederbaum, JCP 111, 2927 (1999)

Burghardt, Nest, Worth, JCP 119, 5364 (2003)

Variationally optimized dynamics

$$\Psi(\mathrm{r}_1,\ldots,\mathrm{r}_P,t)=\sum_{j_1}\cdots\sum_{j_P}A_{j_1\ldots j_P}(t)\prod_{\kappa=1}^{M}\varphi_{j_\kappa}^{(\kappa)}(\mathrm{r}_\kappa,t)\prod_{\kappa=M+1}^{P}g_{j_\kappa}^{(\kappa)}(\mathrm{r}_\kappa,t)$$

$$g_j^{(\kappa)}(\mathrm{r}_\kappa,t)=\exp\left[\mathrm{r}_\kappa\cdot\mathrm{a}_j^{(\kappa)}(t)\cdot\mathrm{r}_\kappa+\boldsymbol{\xi}_j^{(\kappa)}(t)\cdot\mathrm{r}_\kappa+\eta_j^{(\kappa)}(t)\right]$$

multidimensional Gaussian functions*
with time-dependent parameters: $\Lambda_j^{(\kappa)}=\{a_j^{(\kappa)},\boldsymbol{\xi}_j^{(\kappa)},{\eta_j}^{(\kappa)}\}$

Dirac-Frenkel variational principle:

$$\langle\delta\Psi|H-i\frac{\partial}{\partial t}|\Psi\rangle=0$$

⟶ **dynamical equations**

***Note: for on-the-fly applications, use Gaussians only!**

Dynamical equations

Burghardt, Meyer, Cederbaum, JCP 111, 2927 (1999)

$$i\dot{\boldsymbol{A}}^{(s)} = \left(\boldsymbol{S}^{(s)}\right)^{-1}\left[\sum_{s'} \boldsymbol{H}^{(ss')} - i\boldsymbol{\tau}^{(s)}\,\boldsymbol{\delta}(s-s')\right]\boldsymbol{A}^{(s')}$$

$$i\dot{\boldsymbol{\varphi}}^{(\kappa,s)} = \left(1-\hat{\boldsymbol{P}}^{(\kappa,s)}\right)\left[\boldsymbol{\rho}^{(\kappa,s)}\right]^{-1}\sum_{s'}\hat{\boldsymbol{H}}^{(\kappa,ss')}\boldsymbol{\varphi}^{(\kappa,s')}$$

$$i\dot{\boldsymbol{\Lambda}}^{(\kappa,s)} = \left[\boldsymbol{C}^{(\kappa,s)}\right]^{-1}\boldsymbol{Y}^{(\kappa,s)}$$

where $C^{(\kappa,s)}_{j\alpha,l\beta} = \rho^{(\kappa,s)}_{jl}\left(S^{(s,\alpha\beta)}_{jl,\kappa} - \left[S^{(s,\alpha 0)}\left(S^{(s)}\right)^{-1}S^{(s,0\beta)}\right]^{(\kappa,s)}_{jl}\right)$

$$Y^{(\kappa,s)}_{j\alpha} = \sum_{s'}\sum_{l}\left(\langle H^{(\alpha 0,ss')}_{jl,\kappa}\rangle_{jl} - \left[S^{(s,\alpha 0)}\left(S^{(s)}\right)^{-1}\langle H^{(ss')}_{jl}\rangle\right]^{(\kappa,ss')}_{jl}\right)$$

The dynamical equations are non-classical – except if one has a single Gaussian, which evolves according to Newton's equations!

Example: S_2-S_1 CI in pyrazine

Comparison G-MCTDH (full lines) vs. MCTDH (dotted lines)

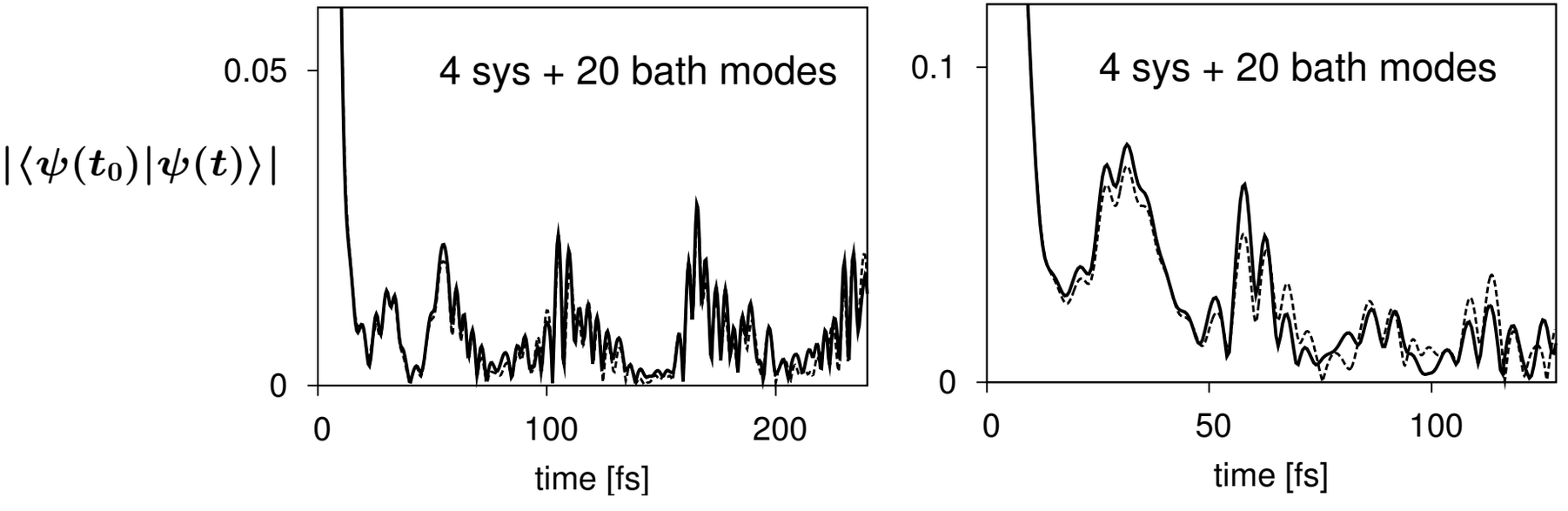

linear CI model **quadratic CI model**

G-MCTDH (i) converges towards the "exact" dynamics, and
(ii) permits approximations + an on-the-fly implementation

Burghardt, Nest, Worth, JCP 119, 5364 (2003); Worth, Robb, Burghardt, Faraday Discuss. 127, 307 (2004)

MCTDH = High-precision tool for $\leq$ 100 dof's

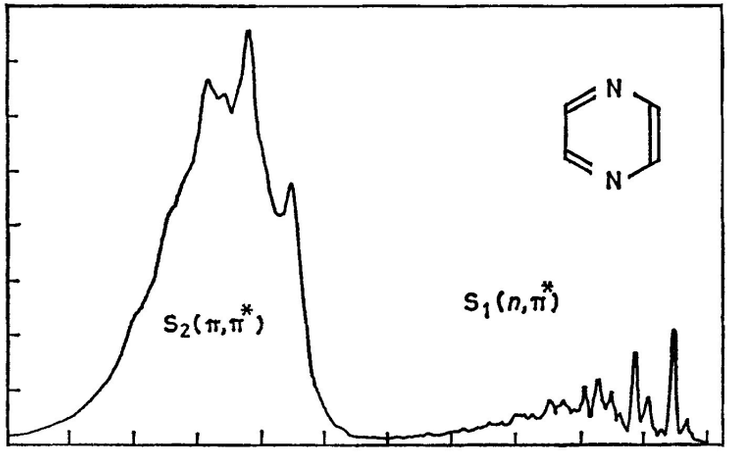

"diffuse" spectral structures

Yamazaki et al., Faraday Discuss. 75, 395 (1983)

$|\langle\psi(t_0)|\psi(t)\rangle|$

FT

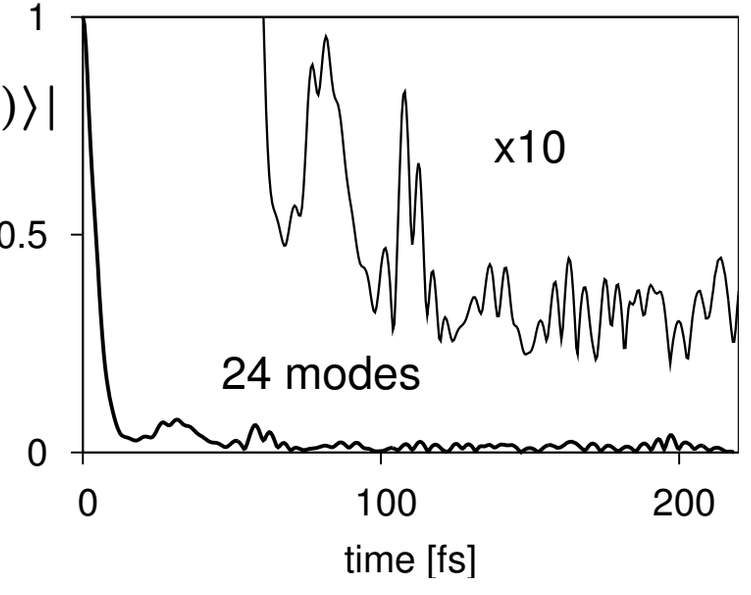

But: Often a highly detailed knowledge on long time scales is not required

What is the right approximation on short time scales?

Strategy 2: Effective-mode models

Reduced-dimensionality models for large systems

$$H = \sum_{i=1}^{N} H_0^{(i)} + \begin{pmatrix} \kappa_i^{(1)}\, x_i & \lambda_i x_i \\ \lambda_i x_i & \kappa_i^{(2)}\, x_i \end{pmatrix} \xrightarrow{\;?\;} H_{\text{eff}} = \sum_{i=1}^{n_{\text{eff}}} \tilde{H}_0^{(i)} + \begin{pmatrix} K_i^{(1)}\, X_i & \Lambda_i X_i \\ \Lambda_i X_i & K_i^{(2)}\, X_i \end{pmatrix}$$

N potentially very large!

n_{eff} small

- approximation should be valid on short time scales
- X_i's are collective modes, or generalized reaction coordinates

Example: high-dimensional avoided crossing

e.g., "tuning" of energy gap by many modes

$$\text{1D crossing} + \sum_{i=1,N} \begin{pmatrix} \kappa_i\, x_i & 0 \\ 0 & -\kappa_i\, x_i \end{pmatrix} + H^{(0)}$$

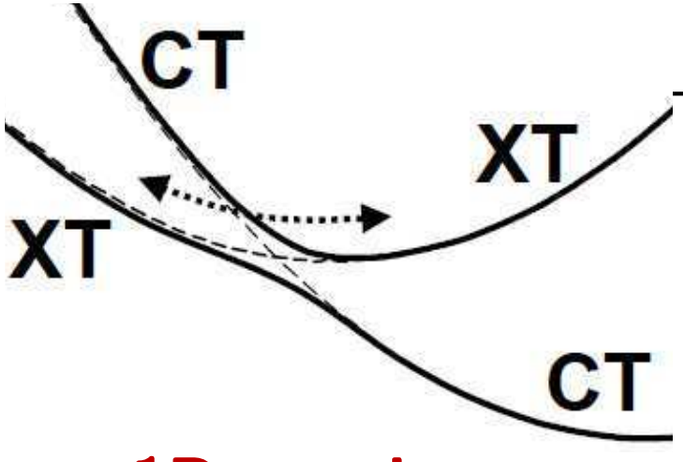

1D crossing

$$\longrightarrow \underbrace{\text{1D crossing} + \begin{pmatrix} \kappa_{\text{eff}} X_{\text{eff}} & 0 \\ 0 & -\kappa_{\text{eff}} X_{\text{eff}} \end{pmatrix}} + \tilde{H}_{N-1}$$

short time dynamics exact

via 1 effective mode

("Brownian oscillator" type model)

General conical intersection: three effective modes

$$H = \sum_i H_i = \sum_i \frac{\omega_i}{2}\left(p_i^2 + x_i^2\right) + V_i^{\text{lin}} \qquad V_i^{\text{lin}} = \frac{1}{2}\kappa_i^{(+)}\, x_i + \begin{pmatrix} \frac{1}{2}\kappa_i^{(-)}\, x_i & \lambda_i x_i \\ \lambda_i x_i & -\frac{1}{2}\kappa_i^{(-)}\, x_i \end{pmatrix}$$

shift + energy gap + coupling

$$X_+ = \sum_i \kappa_i^{(+)}\, x_i \qquad X_- = \sum_i \kappa_i^{(-)}\, x_i \qquad X_\Lambda = \sum_i \lambda_i\, x_i$$

The potential simplifies:

$$\sum_i V_i^{\text{lin}} = \frac{1}{2}X_+ + \begin{pmatrix} \frac{1}{2}X_- & X_\Lambda \\ X_\Lambda & -\frac{1}{2}X_- \end{pmatrix}$$

cf. Atchity & Xantheas & Ruedenberg (1999): (X_-, X_Λ) span the branching plane

Topology and dynamics

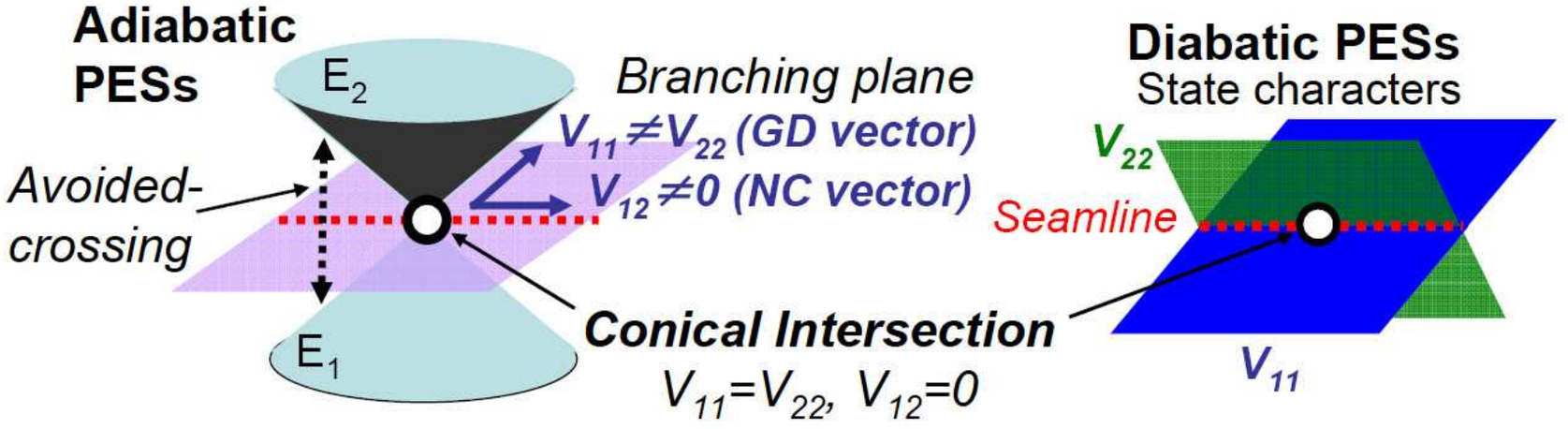

$$\boldsymbol{E}_{\text{adiabatic}} = \boldsymbol{U}^{\boldsymbol{T}} \boldsymbol{V}_{\text{diabatic}} \boldsymbol{U} \; ; \quad \boldsymbol{V}_{\text{diabatic}} = \begin{pmatrix} \boldsymbol{V_{11}} & \boldsymbol{V_{12}} \\ \boldsymbol{V_{12}} & \boldsymbol{V_{22}} \end{pmatrix} = \frac{\boldsymbol{1}}{\boldsymbol{2}} \boldsymbol{X}_{+} + \begin{pmatrix} \frac{1}{2}\boldsymbol{X}_{-} & \boldsymbol{X}_{\Lambda} \\ \boldsymbol{X}_{\Lambda} & -\frac{1}{2}\boldsymbol{X}_{-} \end{pmatrix}$$

- **two intrinsic modes (X_-, X_Λ) along which the degeneracy is lifted**
- **three intrinsic modes (X_+, X_-, X_Λ) reproduce the short-time dynamics**

Construction of orthogonal effective modes

transformation $(\{x_S\}, x_{1_B} \ldots x_{N_B}) \longrightarrow (\{x_S\}, X_1, X_2, X_3, X_4 \ldots X_{N_B})$

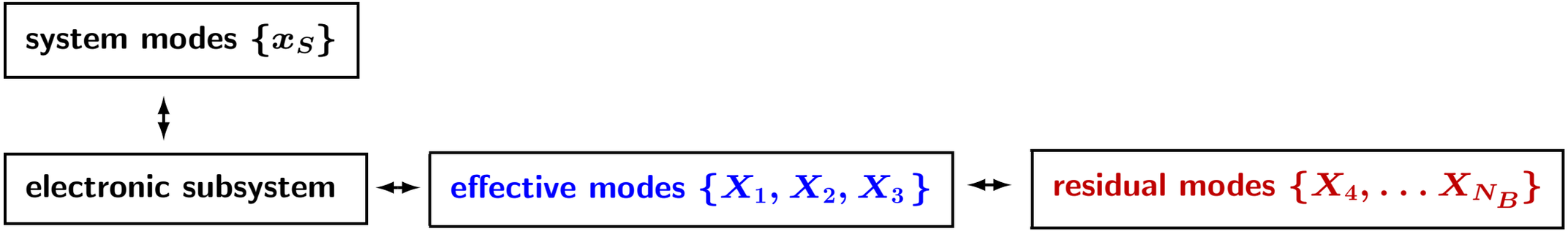

short-time, "inertial" dynamics

intermediate and long time dynamics

$$H_S(\{x_S\}) + H_{\text{eff}}(X_1, X_2, X_3)$$

describes all short-time effects exactly!
(i.e., the first few moments of the Hamiltonian, $\langle 0|H^n|0\rangle$ are reproduced.)

Cederbaum, Gindensperger, Burghardt, Phys. Rev. Lett., 94, 113003 (2005), Burghardt, Gindensperger, Cederbaum, Mol. Phys., 104, 1081 (2006), Gindensperger, Burghardt, Cederbaum, J. Chem. Phys. 124, 144104, 144105 (2006)

Construction of orthogonal effective modes, cont'd

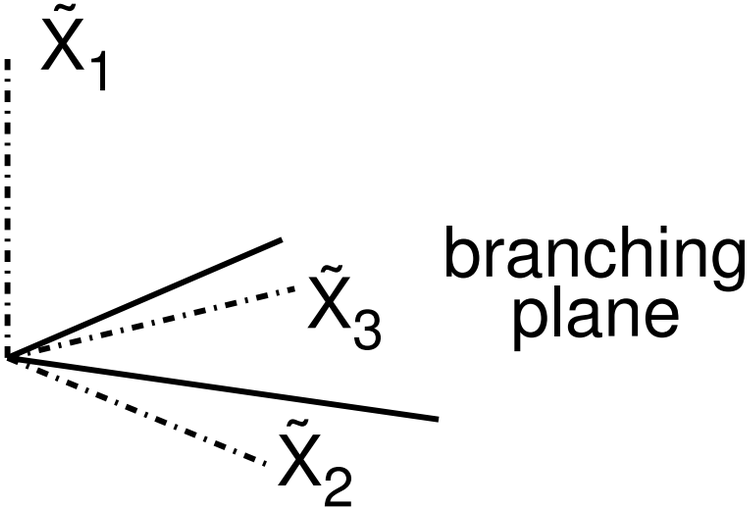

$$\begin{pmatrix} X_1 \\ X_2 \\ X_3 \end{pmatrix} = \begin{pmatrix} T_{11} & T_{12} & 0 \\ T_{21} & T_{22} & 0 \\ T_{31} & T_{32} & T_{33} \end{pmatrix} \begin{pmatrix} X_+ \\ X_- \\ X_\Lambda \end{pmatrix}$$

Cederbaum, Gindensperger, Burghardt, Phys. Rev. Lett. 94, 113003 (2005).

or:

seam coordinate

branching plane coordinates

$$\begin{pmatrix} \tilde{X}_1 \\ \tilde{X}_2 \\ \tilde{X}_3 \end{pmatrix} = \begin{pmatrix} \tilde{T}_{11} & \tilde{T}_{12} & \tilde{T}_{13} \\ 0 & \tilde{T}_{22} & \tilde{T}_{23} \\ 0 & \tilde{T}_{32} & \tilde{T}_{33} \end{pmatrix} \begin{pmatrix} X_+ \\ X_- \\ X_\Lambda \end{pmatrix}$$

cf. Yarkony's (g,h,s) vectors!

Burghardt, Gindensperger, Cederbaum, Mol. Phys., 104, 1081 (2006).

Additional transformations of the residual bath

⟶ hierarchy of modes within the residual space

effective modes + chain(s) of residual modes:

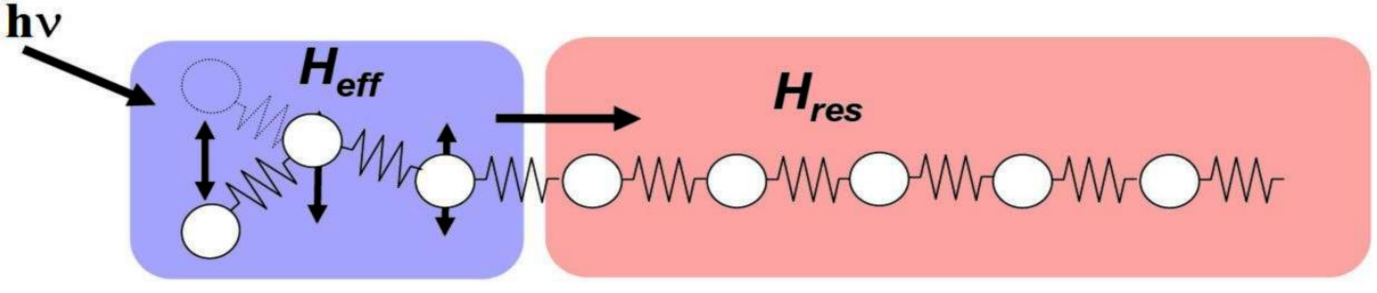

- cf. Rubin model, Mori continued fractions, Adelman (MTGLE), . . .
- construct a chain in such a way that truncation at the order n (i.e., $3n+3$ modes) conserves the Hamiltonian moments (cumulants) up to the $(2n+3)$rd order

Hierarchical electron-phonon (HEP) model

$$\hat{H}^{(n)} = \hat{H}_{\rm eff} + \sum_{l=1}^{n} \hat{H}^{(l)}_{\rm res}$$

$$\hat{H}^{(l)}_{\rm res} = \sum_{i=3l+1}^{3l+3} \frac{\Omega_i}{2}(\hat{P}_i^2 + \hat{X}_i^2)\hat{1} + \sum_{i=3l+1}^{3l+3} \sum_{j=i-3}^{i-1} d_{ij}\left(\hat{P}_i\hat{P}_j + \hat{X}_i\hat{X}_j\right)\hat{1}$$

$$d = \begin{pmatrix}
d_{11} & d_{12} & d_{13} & d_{14} & & & & & & \\
d_{21} & d_{22} & d_{23} & d_{24} & d_{25} & & & & & \\
d_{31} & d_{32} & d_{33} & d_{34} & d_{35} & d_{36} & & & & \\
d_{41} & d_{42} & d_{43} & d_{44} & d_{45} & d_{46} & d_{47} & & & \\
 & d_{52} & d_{53} & d_{54} & d_{55} & d_{56} & d_{57} & d_{58} & & \\
 & & d_{63} & d_{64} & d_{65} & d_{66} & d_{67} & d_{68} & d_{69} & \\
 & & & d_{74} & d_{75} & d_{76} & d_{77} & d_{78} & d_{79} & \cdots \\
 & & & & d_{85} & d_{86} & d_{87} & d_{88} & d_{89} & \cdots \\
 & & & & & d_{96} & d_{97} & d_{98} & d_{99} & \cdots \\
 & & & & & & \vdots & \vdots & \vdots &
\end{pmatrix}$$

band-diagonal form via Jacobi/Givens type transformation

Burghardt, Tamura,
CCP6 Proceedings 2006
Tamura, Bittner, Burghardt,
JCP 126, 021103 (2007)
cf. Gindensperger et al.
JCP 126, 034106 (2007)

Example: butatriene cation

$[C{=}C{=}C{=}C]^+$ D_1/D_0 CI

2 system + 20 bath modes → 2 system + 3 effective modes

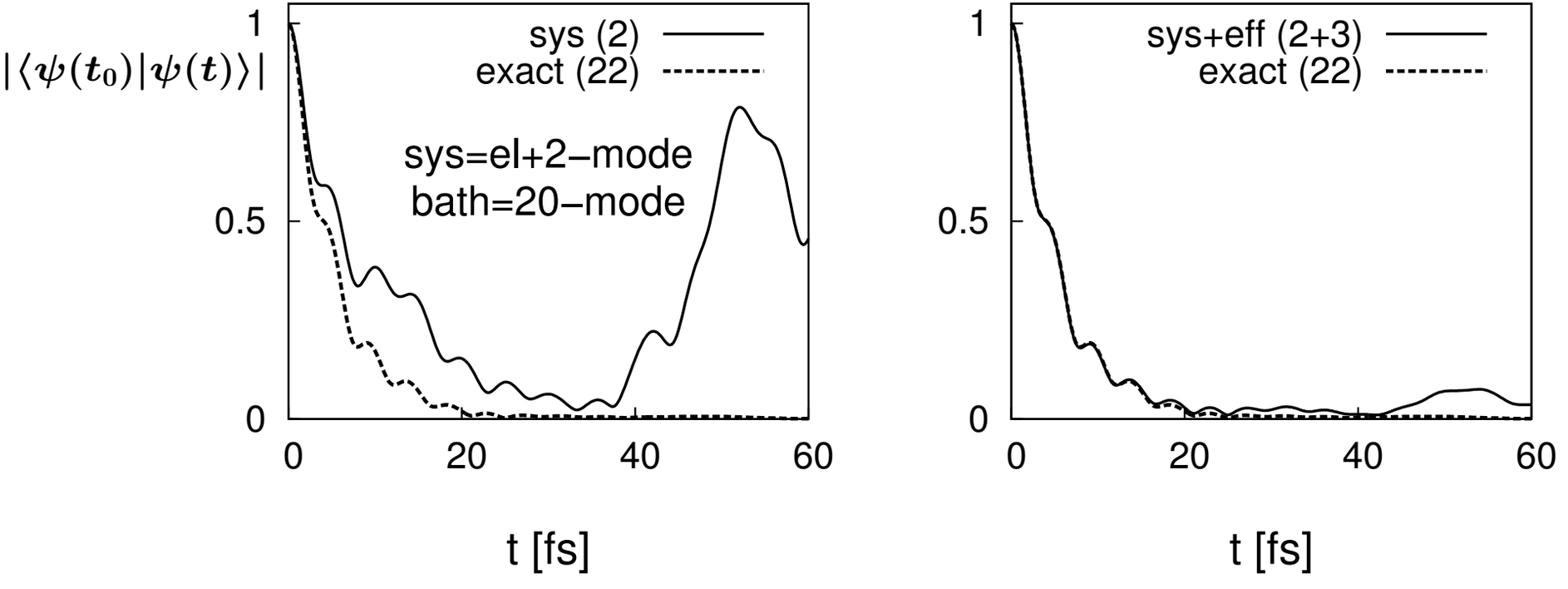

Burghardt et al., Mol. Phys., 104, 1081 (2006), Gindensperger et al., J. Chem. Phys. 124, 144105 (2006)

- **Introduction:**
  Photophysics of organic semiconductors

- **Phonon-driven electronic processes in many dimensions:**
  Conical intersections and effective-mode models

- **Ultrafast exciton dissociation at polymer heterojunctions:**
  A molecular, quantum-dynamical perspective

Photoinduced processes at polymer heterojunctions

TFB:F8BT heterojunction

Tamura, Bittner, Burghardt
JCP 126, 021103 (2007)

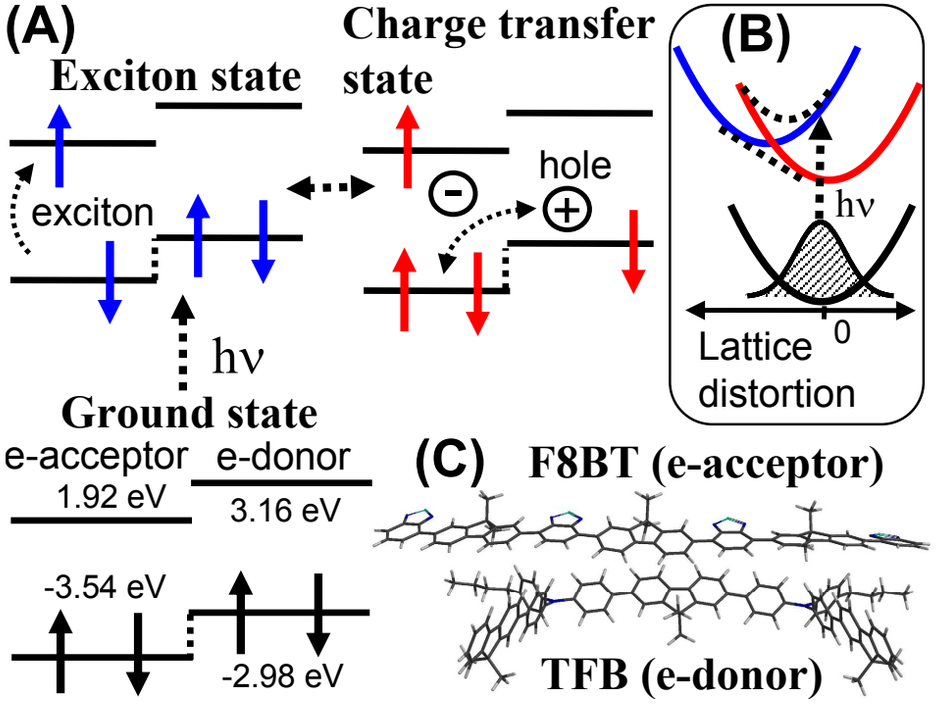

- initial photogeneration of an exciton state ("bright" state)
- exciton decay to an interfacial charge transfer state (exciplex)
- possible exciton regeneration at the heterojunction

Exciton decay at a TFB:F8BT heterojunction

Exciton ⟶ charge transfer state ("exciplex") nonadiabatic transition

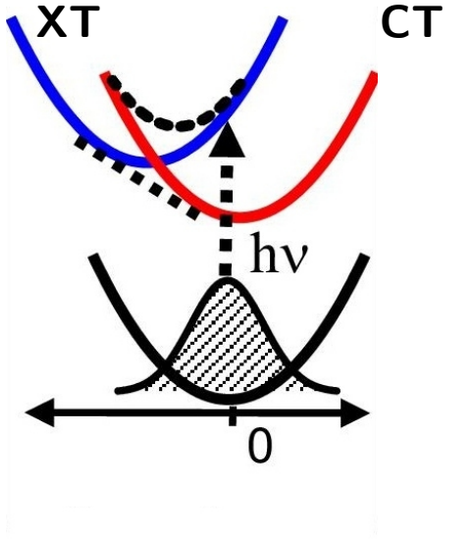

2-state electron-phonon coupling model:

$$H = \sum_{i}^{N=24} H_i = \sum_i \frac{\omega_i}{2}\left(p_i^2 + x_i^2\right) + V_i^{\text{lin}}$$

$$V_i^{\text{lin}} = \begin{pmatrix} \kappa_i^{(1)} x_i & \lambda_i x_i \\ \lambda_i x_i & \kappa_i^{(2)} x_i \end{pmatrix}$$

parameterization for polymer dimer; semi-empirical (PM3) calculations + Wannier-function representation

Bittner et al., JCP 122, 214719 (2005)

state 1 = exciton (XT) state
state 2 = charge transfer (CT) state

"phonon bath": C=C stretch, ring torsional modes

A. Pereverzev and E. R. Bittner, J. Chem. Phys. (2006)

Phonon bath and effective-mode construction

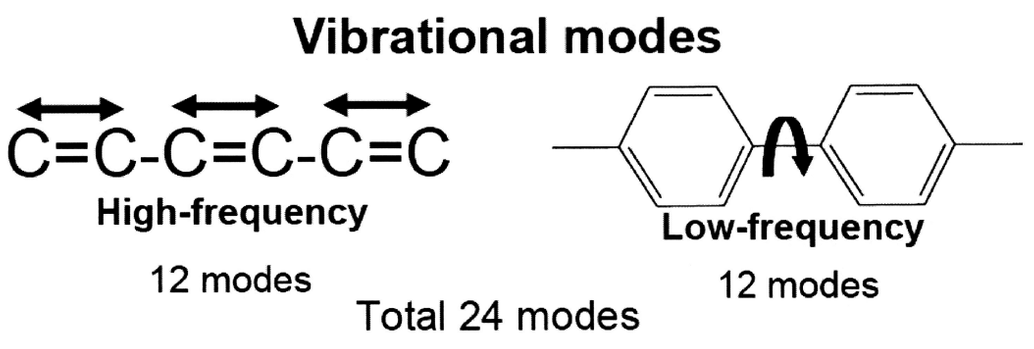

The effective/residual-mode hierarchy features the high- vs. low-frequency branches in alternation:

(X_1, X_2, X_3): high-frequency

(X_4, X_5, X_6): low-frequency

(X_7, X_8, X_9): high-frequency

XT/CT nonadiabatic coupling region

representation in the branching space coordinates (X_1, X_2)
(both of high-frequency, C=C stretch type)

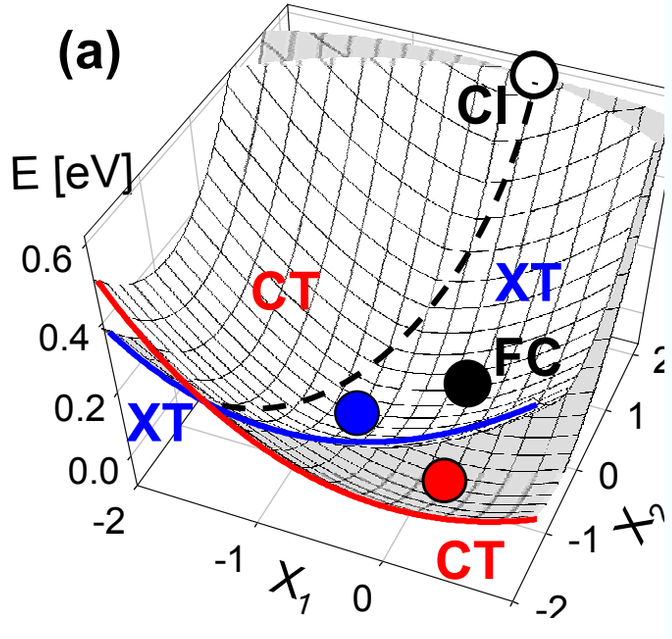

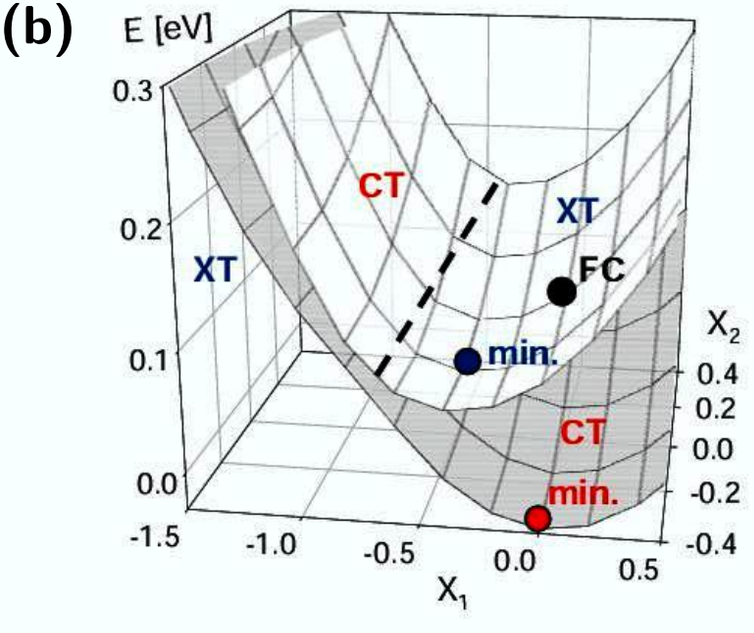

The dynamics happens "below" a conical intersection

Exact dynamics vs. effective-mode approximation

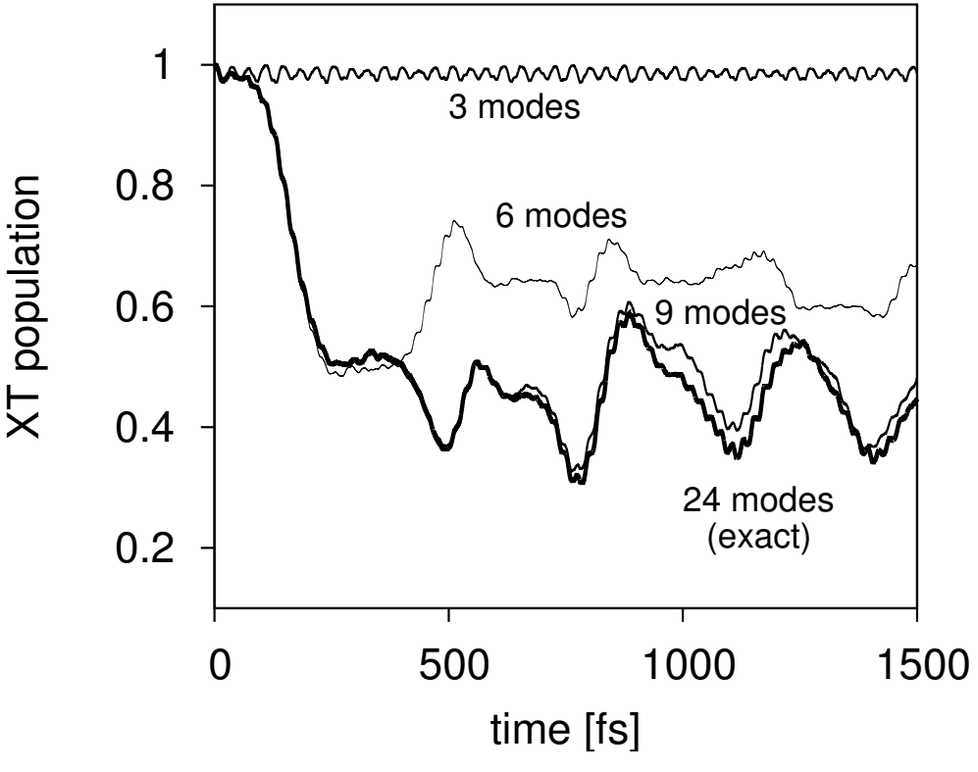

- very fast ($\sim$ 250 fs) decay followed by oscillations (cf. 24 modes = exact)
- 3 effective modes: **not** a good approximation
- 9 effective modes: **very close** to the exact 24-mode result!

The low-frequency (torsional) modes play a crucial role

Decisive role of energy redistribution/dephasing between the phonon branches

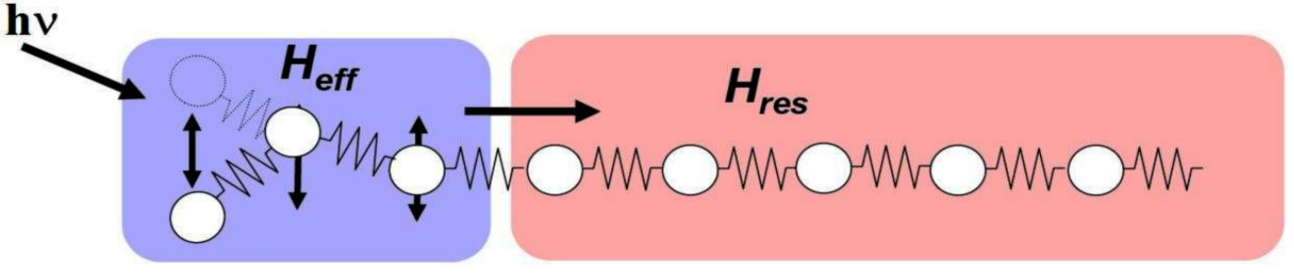

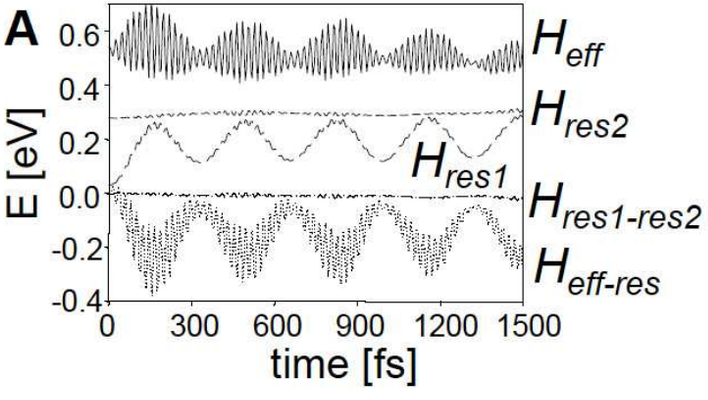

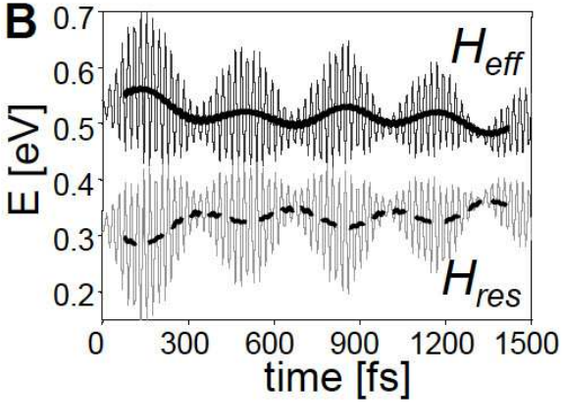

- temperature not included as yet
- but the explicit multi-dimensional phonon bath acts so as to induce dissipation/dephasing

Change of topology due to low-frequency modes:

The branching plane is periodically "shaken" by the low-frequency modes

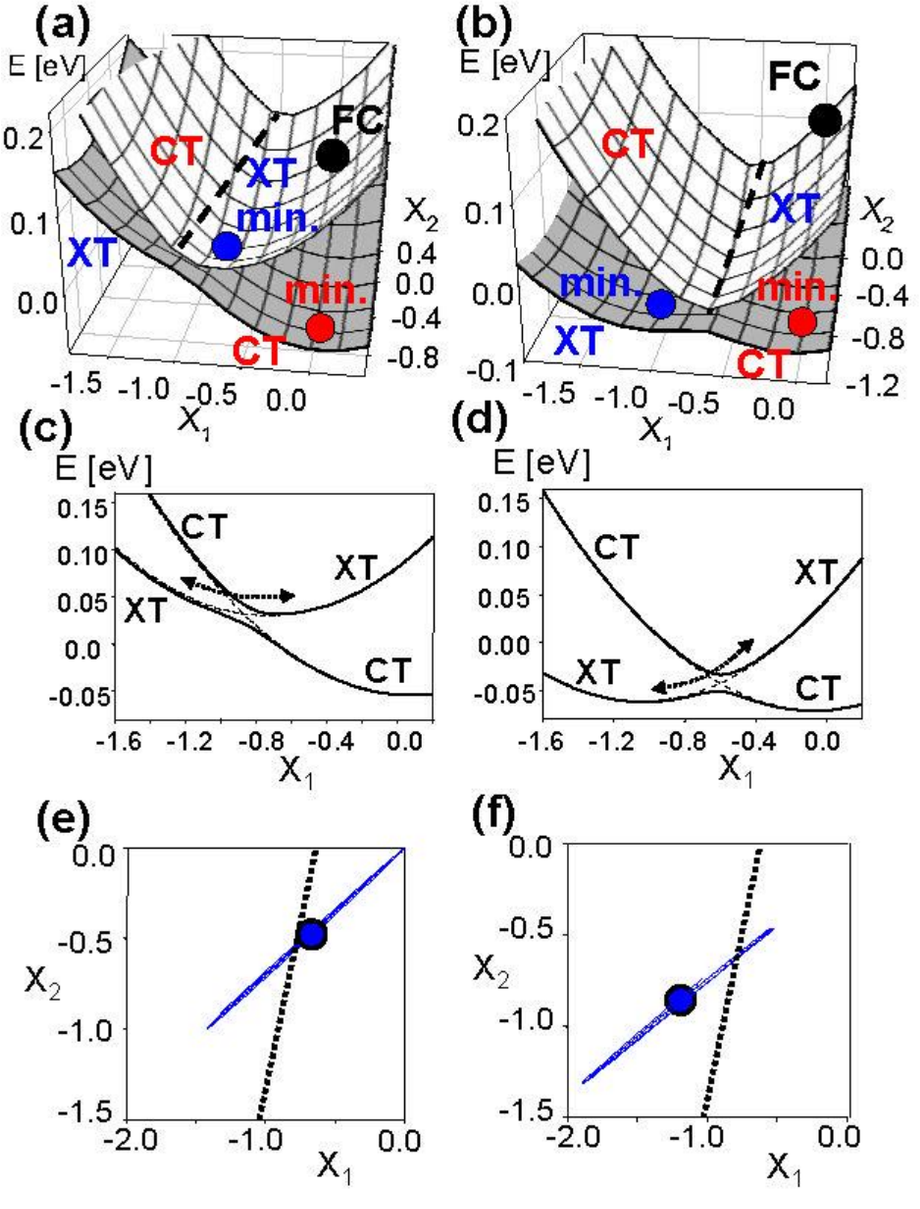

left: $t = 0$ **fs**

right: $t = 150$ **fs**

Combined effective/residual-mode potential

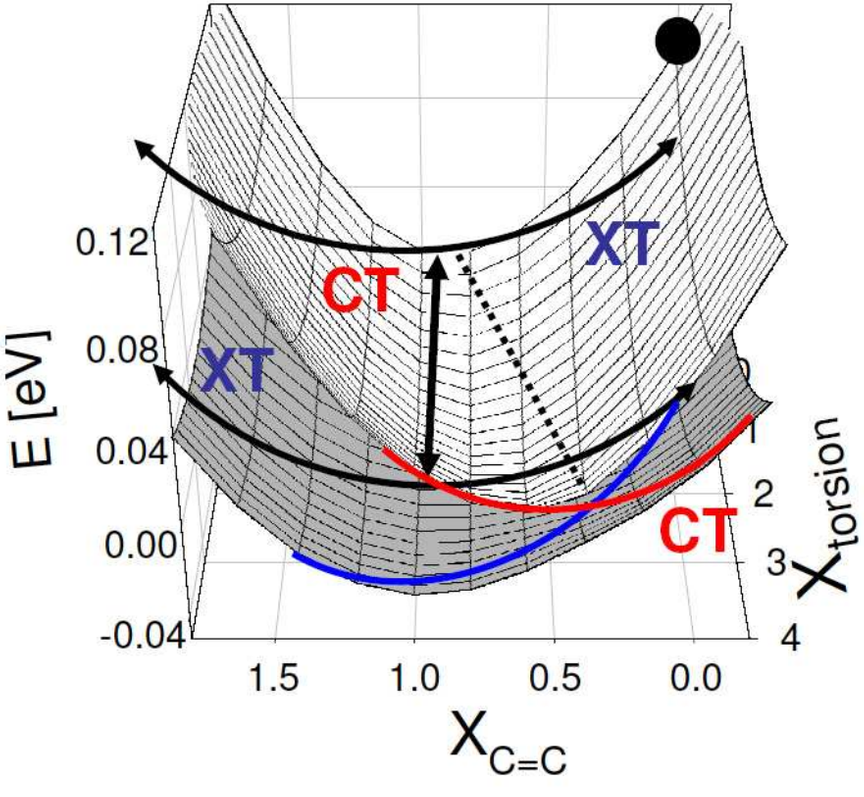

Qualitatively correct model:

branching-plane mode X_1

+ residual mode X_4

= 2D avoided crossing

Dynamics far from equilibrium

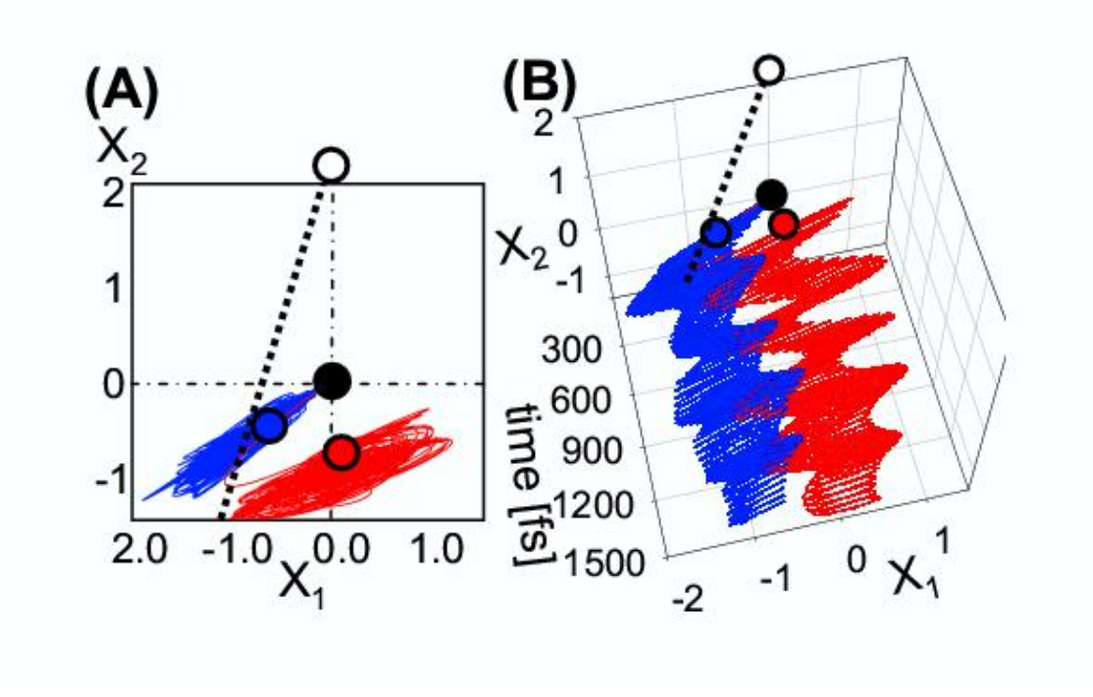

blue: XT red: CT

wavepacket "trajectories" ($\langle X_1 \rangle_t$, $\langle X_2 \rangle_t$): coherent dynamics is dominant

Tamura, Bittner, Burghardt, J. Chem. Phys., 126, 021103 (2007)

Markovian closure of the mode hierarchy

$$\hat{H}^{(n)} = \hat{H}_{\rm eff} + \sum_{l=1}^{n} \hat{H}_{\rm res}^{(l)} + \hat{H}_{\rm Markov}^{(n)}$$

$$\hat{H}_{\rm Markov}^{(n)} = \sum_{i=1}^{N_B} \frac{\omega_{B,i}}{2}(\hat{p}_{B,i}^2 + \hat{x}_{B,i}^2)\hat{1} + \sum_{i=3n+1}^{3n+3}\sum_{j=1}^{N_B} d_{ij}^B \left(\hat{P}_i\hat{p}_j + \hat{X}_i\hat{x}_j\right)\hat{1}$$

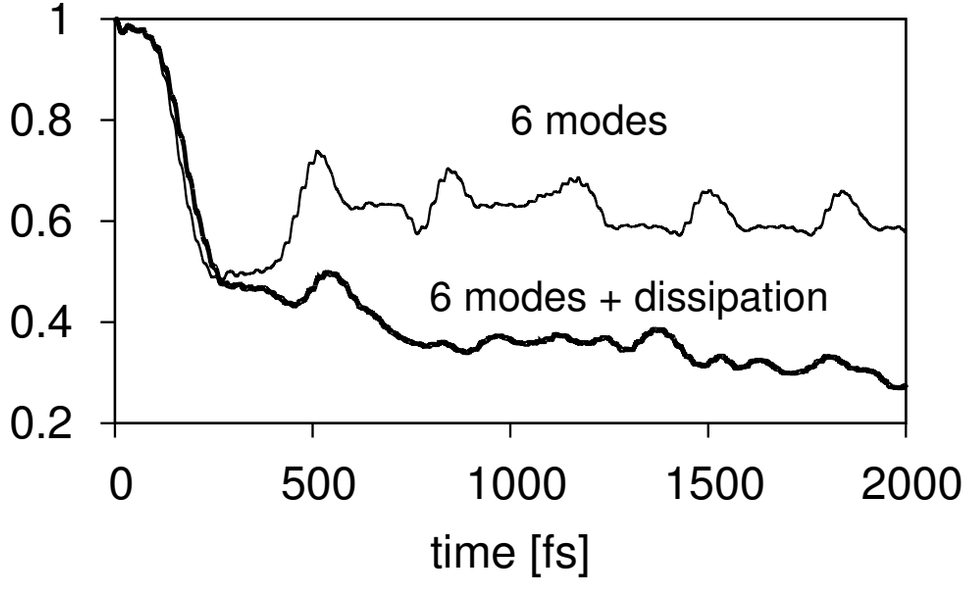

add $N_B = 15$-mode Ohmic bath (resonant with low-frequency modes); here: $T = 0$

Surrogate Liouvillian generators/propagators

+ Markovian closure

$$\hat{\tilde{L}}\hat{\rho}_{S+\mathrm{eff}} = -i[\hat{H}_{\mathrm{eff}}, \hat{\rho}_{S+\mathrm{eff}}] + \hat{\tilde{L}}_{\mathrm{Markov}}\hat{\rho}_{S+\mathrm{eff}}$$

$\hat{\rho}_{S+\mathrm{eff}}$ = reduced density operator in the augmented system + effective-mode space

generalized Brownian oscillator models

Beyond the two-state model

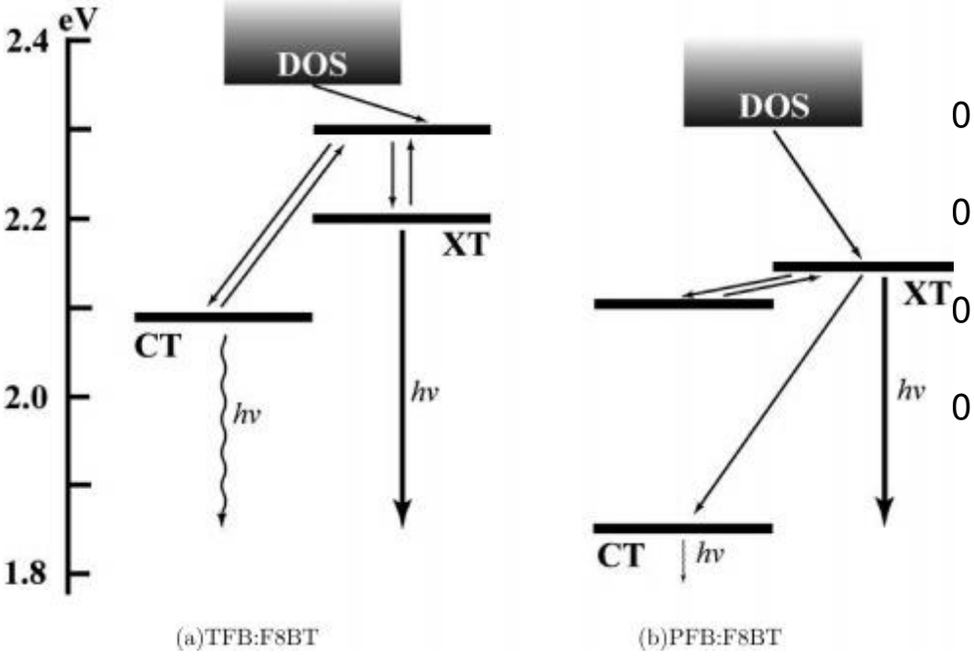

absorption spectrum TFB:F8BT

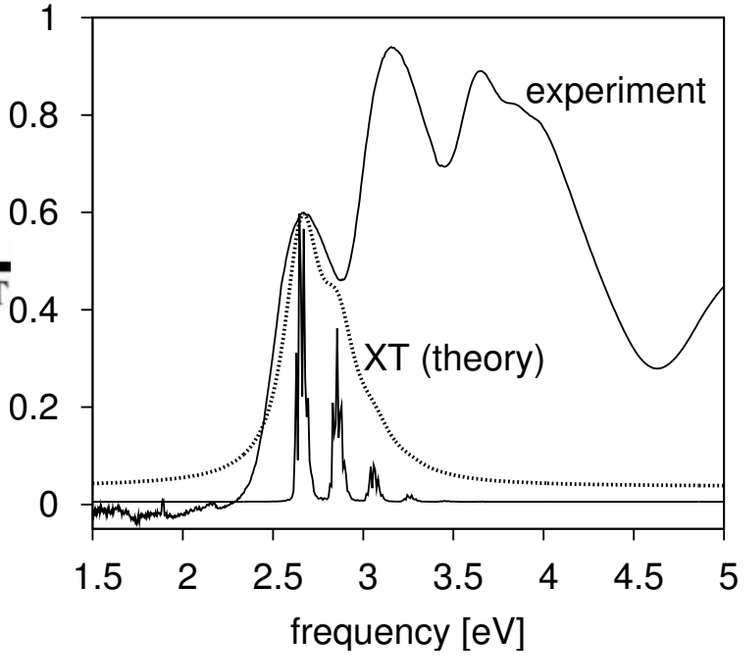

Ramon, Bittner, J. Phys. Chem. 110, 21001 (2006)

Tamura, Bittner, Burghardt, JCP 127, 034706 (2007)

A second CT state might play a non-negligible role

Three-state extension of exciton decay model

Multidimensional landscape of intersecting surfaces

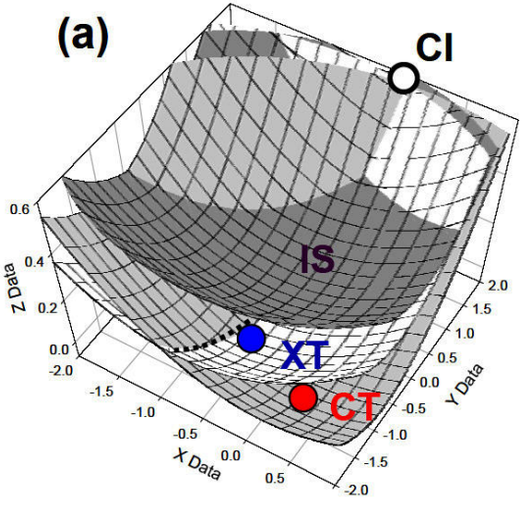

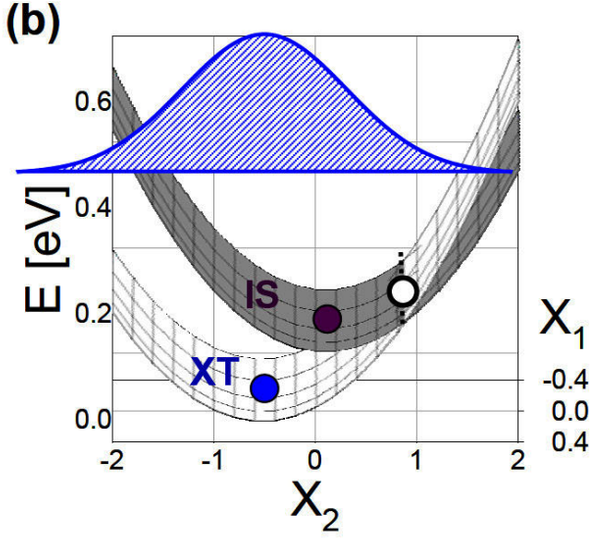

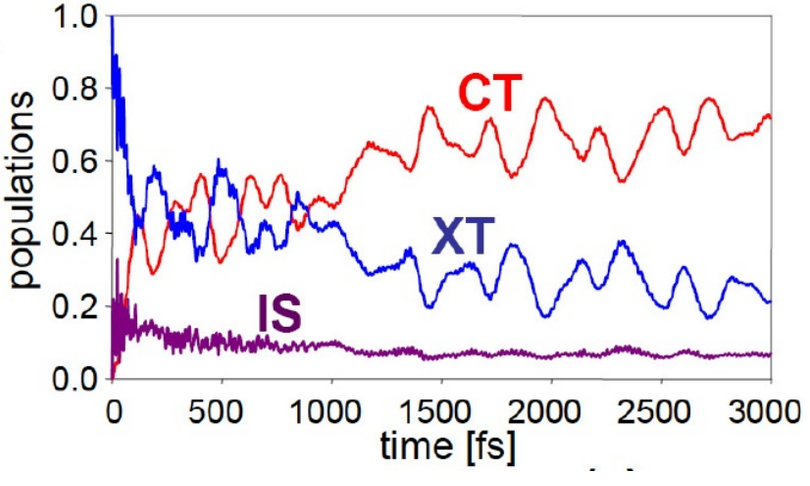

XT = exciton state CT = charge transfer state IS = intermediate state

Tamura, Ramon, Bittner, Burghardt, arXiv:0707.2163 [cond-mat.soft]

Direct vs. indirect XT → CT pathways

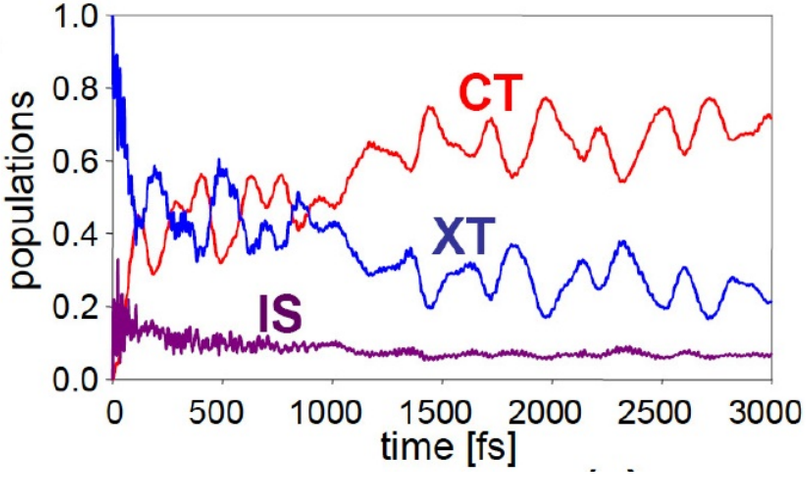

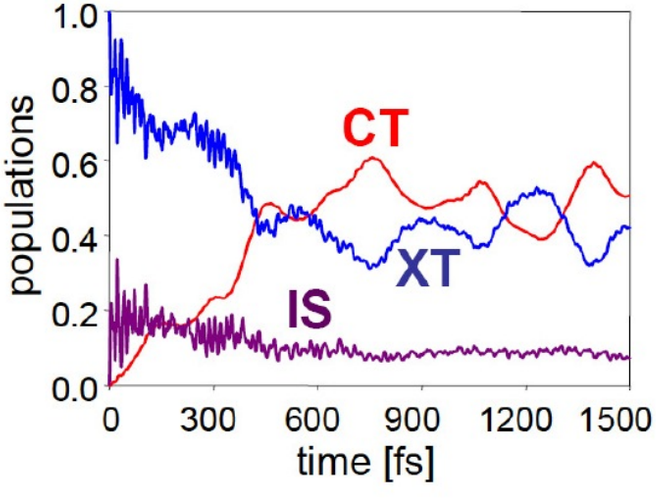

superposition of direct + indirect pathways

only XT → IS → CT

The IS state (and other states) can function as a "bridge"

Extended effective-mode model

$$\boldsymbol{H}_{\text{eff}} = \boldsymbol{H}_0 + \sum_{i=1}^{6} \begin{pmatrix} \boldsymbol{K}_i^{(1)} \boldsymbol{X}_i + \boldsymbol{D}_i \boldsymbol{X}_i & \boldsymbol{\Lambda}_i^{(12)} \boldsymbol{X}_i & \boldsymbol{\Lambda}_i^{(13)} \boldsymbol{X}_i \\ \boldsymbol{\Lambda}_i^{(12)} \boldsymbol{X}_i & \boldsymbol{K}_i^{(2)} \boldsymbol{X}_i - \boldsymbol{D}_i \boldsymbol{X}_i & \boldsymbol{\Lambda}_i^{(23)} \boldsymbol{X}_i \\ \boldsymbol{\Lambda}_i^{(13)} \boldsymbol{X}_i & \boldsymbol{\Lambda}_i^{(23)} \boldsymbol{X}_i & \boldsymbol{K}_i^{(3)} \boldsymbol{X}_i \end{pmatrix} + \text{bilinear couplings}$$

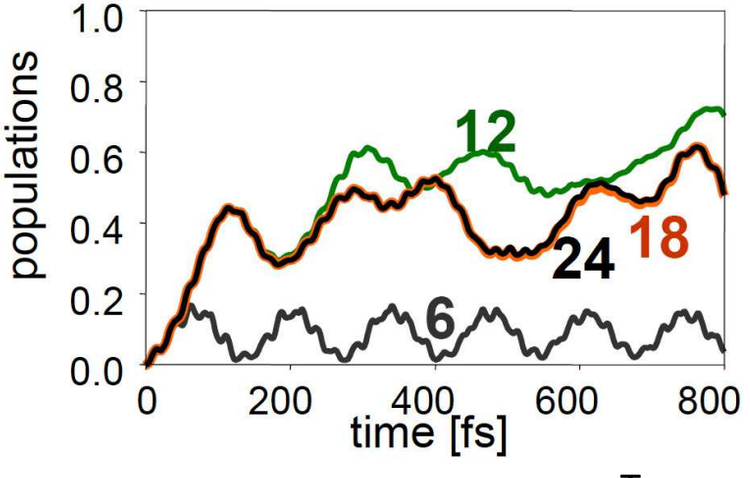

$X_1 \ldots X_6$: high-frequency

$X_7 \ldots X_{12}$: low-frequency

Tamura, Ramon, Bittner, Burghardt, arXiv:0707.2163 [cond-mat.soft]

Different interface configurations

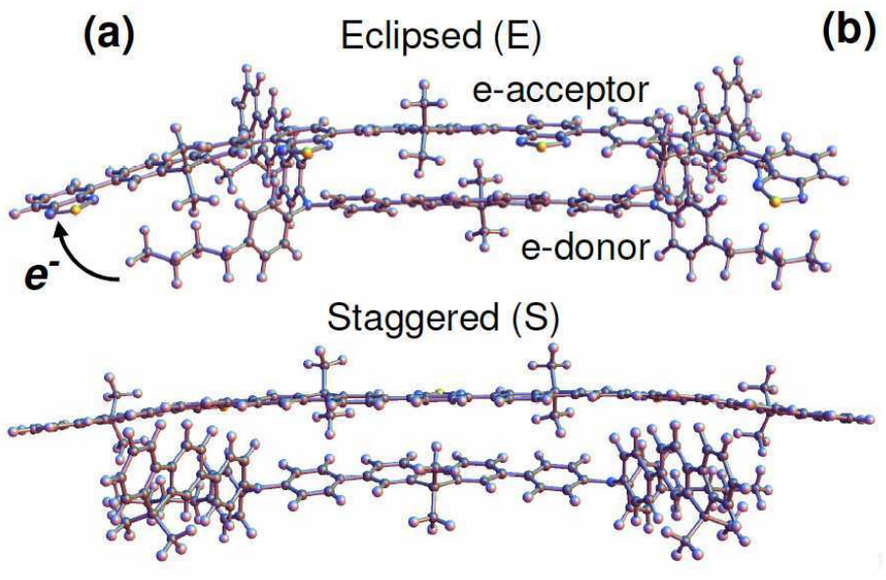

2-state XT/CTmodel

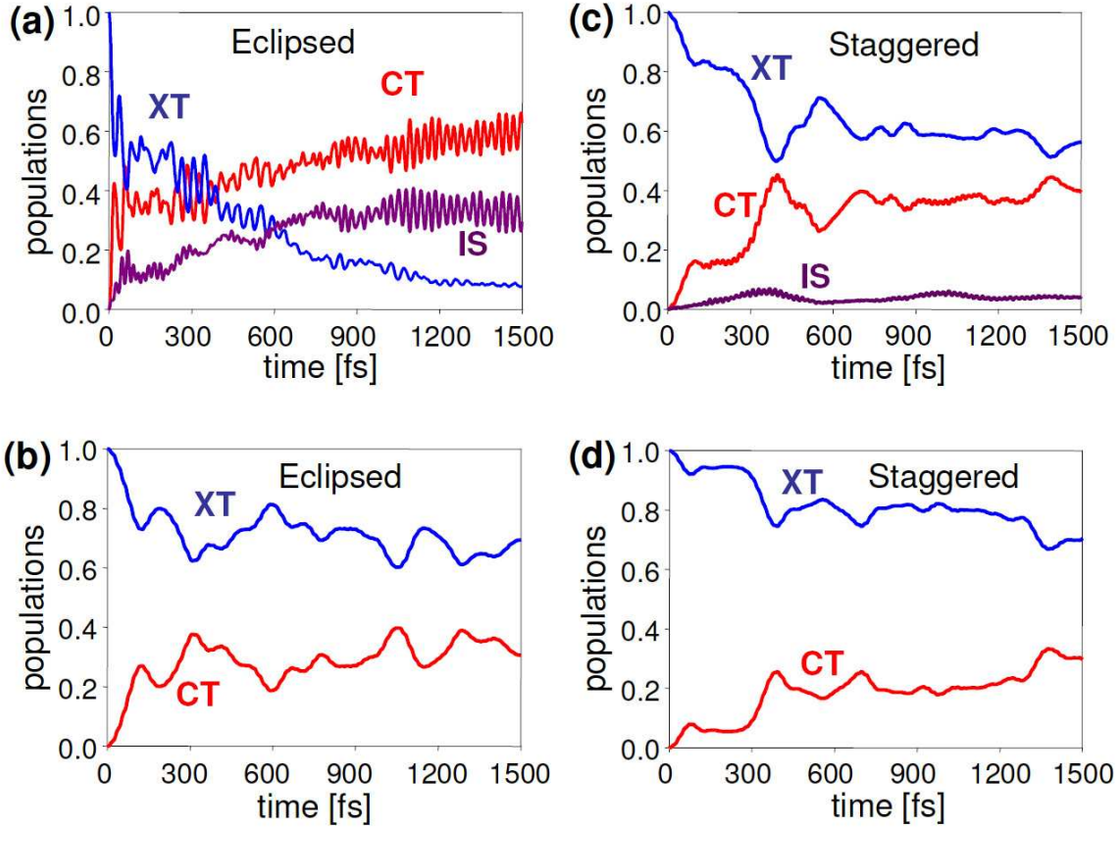

Exciton decay dynamically robust in the presence of intermediate state(s)

Interface configurations: role of stacking

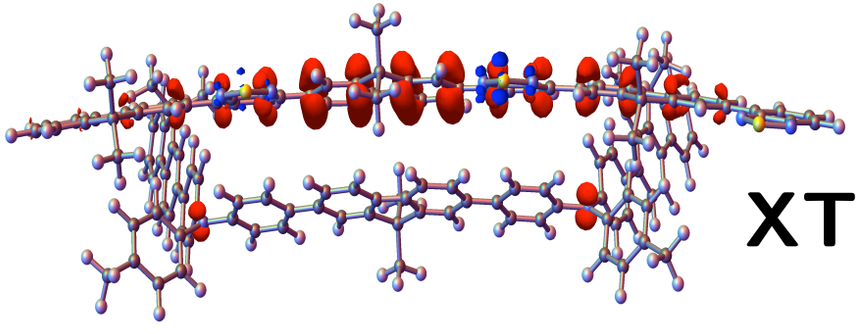

XT

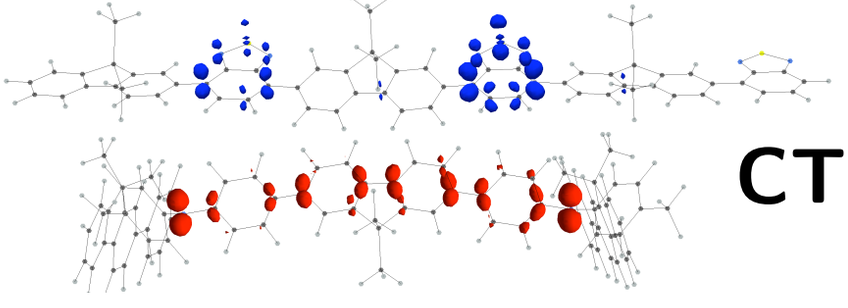

CT

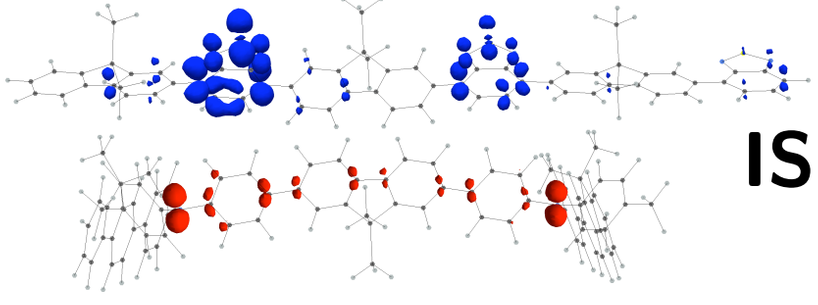

IS

eclipsed:

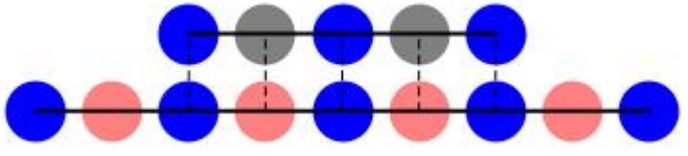

staggered:

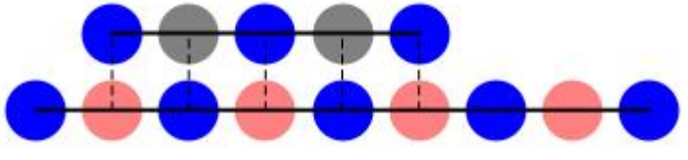

What about site-site hopping?

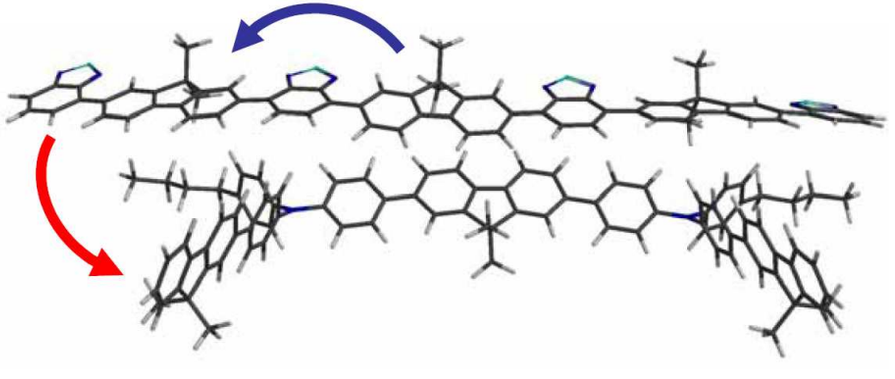

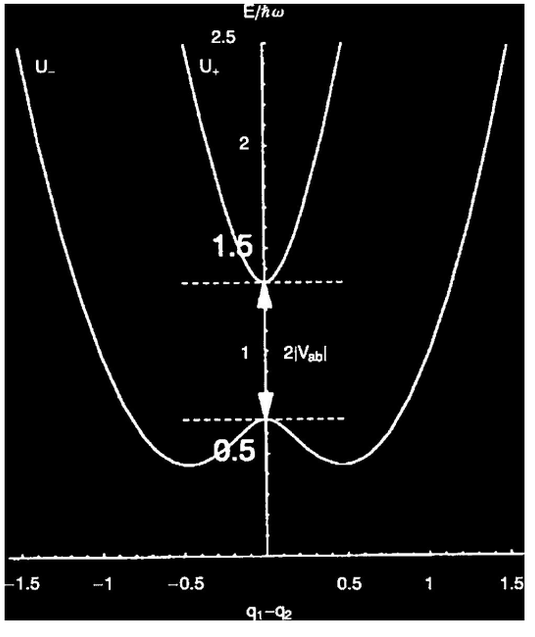

- not included in the model so far
- current assumption: charge separation/recombination occurs "close" to where the photoexcitation takes place (i.e., domain size of the order of the exciton diffusion length)

Conclusions

- LVC model plus HEP hierarchy suitable to describe the ultrafast exciton decay at the heterojunction interface

- Exact quantum dynamical analysis for 2- and 3-state models (parameterized by semiempirical calculations for a 24-mode phonon bath)

- The electron-phonon coupling is dominated by the high-frequency (C=C stretch) modes

- However, the low-frequency (ring torsional) modes are decisive in generating the XT $\longrightarrow$ CT decay

- The ultrafast dynamical processes are far from equilibrium, and cannot be addressed by conventional rate theories (Marcus etc.)

- Results depend on the details of the interface morphology, vibrational frequencies, energy gaps etc. $\longrightarrow$ engineering of these properties

References:

Nonadiabatic dynamics and effective-mode theory:

L. S. Cederbaum, E. Gindensperger, I. Burghardt, Phys. Rev. Lett., 94, 113003 (2005).
I. Burghardt, E. Gindensperger, L. S. Cederbaum, Mol. Phys., 104, 1081 (2006).
E. Gindensperger, I. Burghardt, L. S. Cederbaum, J. Chem. Phys. 124, 144104 (2006).
E. Gindensperger, I. Burghardt, L. S. Cederbaum, J. Chem. Phys. 124, 144105 (2006).
I. Burghardt, in: "Quantum dynamics of Complex Molecular Systems", Springer (2006).

Exciton dissociation at a polymer heterojunction:

H. Tamura, E. R. Bittner, I. Burghardt, J. Chem. Phys., 126, 021103 (2007).
H. Tamura, E. R. Bittner, I. Burghardt, J. Chem. Phys., 127, 034706 (2007).
H. Tamura, J. G. S. Ramon, E. R. Bittner, I. Burghardt, arXiv:0707.2163 [cond-mat.soft].

Thanks to:

CNRS, ANR (France) for financial support